Supporting Information

Constructing covalent organic frameworks with dense thiophene S sites for effective iodine capture

Yiling Ran[1,2,3], Yi Wang[3], Man Yang[3], Jian Li[3], Yan Zhang[1*], Zhanguo Li[3*]

1 School of Chemistry, Southwest Jiaotong University, Chengdu, Sichuan 610031, China

2 School of Life Science and Engineering, Southwest Jiaotong University, Chengdu Sichuan 610031, China

3 State Key Laboratory of NBC Protection for Civilian, 102205 Beijing, China

*Corresponding author:

lizhanguo@sklnbcpc.cn (Zg.Li)

zyzw@swjtu.edu.cn (Y.Zhang)

1. Experimental section

1.1 Materials

Benzo[1,2-b:3,4-b':5,6-b"]trithiophene-2,5,8-tricarbaldehyde (BTT)) from Shanghai Acmec Biochemical Technology Co., LTD., Acetic acid (HAc), o-dichlorobenzene (o-DCB), n-BuOH, N, N-dimethylformamide (DMF), methanol (MeOH), ethanol (EtOH) and cyclohexane are from Shanghai McLean Biochemical Technology Co., LTD., 1,3,5-tris-(4-aminophenyl) triazine (TAPT), 1,3,5-tris(4-aminophenyl) benzene (TAB), and iodine come from Shanghai Aladdin Biochemical Technology Co., LTD. All aqueous solutions are prepared by a deionized water mechanism. All reagents are analytical grade and can be used without further purification.

1.2 Synthesis of TAPT-COF and TAB-COF

TAPT (72.1 mg, 0.2 mmol) or TAB (70.3 mg, 0.2 mmol) and BTT (66.1 mg, 0.2 mmol) was filled into the Schlenk tube, followed by the addition of 6.3 ml mixed solvent of n-BuOH/o-DCB/ 6 M HOAc (volume ratio 10/10/1). The mixture was sonicated for 15 min; then the tube was degassed by three freeze-pump thaw cycles under 77 K liquid nitrogen. Subsequently, the Schlenk tube was heated at 120℃ for 4 d. After cooled to room temperature, the synthesized materials were obtained by filtration and washed with N, N-dimethylformamide, methanol, and ethanol several times. TAPT-COF and TAB-COF were in a vacuum at 60℃ for 12 h.

1.3 Iodine vapor capture experiment

Three pre-weighed 5 ml open glass vials were placed in a 100 ml glass container. COF materials were placed in one of the vials, I_2 (500 mg) was placed in a second vial, and the third vial was used for blank control. Then, the glass container was placed in a heated oven at 75℃. After a certain contact time, remove the glass container from the oven and cooled to room temperature. The vial containing the COF materials was measured. Then, the vial returned to the glass container and continued to absorb iodine until the weight of the bottles did not change. Three parallel tests were used to reduce the experimental error. The adsorption amount is calculated using the following formula.

$$Q_t(g/g) = \frac{(M_t - M_0) - (m_t - m_0)}{M_0}$$

Where, Q_t is the adsorption quantity at time t, M_t is the mass of the adsorbent at time t, M_0 is the mass of the adsorbent at time initial, m_t is the mass of the blank control vial at time t, m_0 is the mass of the blank control vial at time initial.

1.4 Cyclohexane-iodine solution adsorption experiment

TAPT-COF and TAB-COF were dispersed in the solution containing 250 mg/L iodine/cyclohexane solution (solid-liquid ratio 1g/L) at room temperature. Every once in a while, 1 mL solution was taken by filtration and measured with an UV spectrophotometer at the wavelength of 523 nm (0 h, 0.5 h, 1 h, 2 h, 4 h, 6 h, 8 h, 10 h, 24 h), and the corresponding concentration was calculated according to the standard curve.

1.5 COFs retention test

A certain amount of the iodine-adsorbed COF materials were placed in an open glass vial and the vial was placed in an empty large vial. After one day at room temperature and atmospheric pressure, the weight of the vial containing the iodine-adsorbed COF material was recorded, and the vial was returned to the empty larger vial, which was opened and left for seven days. The accidental error was reduced by three parallel experiments.

1.6 Recycle experiment of iodine adsorption by COFs

The I_2-saturated COF powder was washed with ethanol to release iodine. The COF powder was collected by centrifugation and dried overnight in a vacuum at 80℃. The dried samples were used for the next iodine adsorption experiment. Then, the washing-drying-iodine adsorption process was repeated four times. The accidental error was reduced by three parallel experiments.

1.7 Kinetics analysis

The pseudo-first-order and pseudo-second-order kinetic models were used to study the adsorption kinetics of iodine vapor and solution. The kinetic models were calculated using the following formulas.

Pseudo- first-order kinetic: $$\ln\left(q_e - q_t\right) = lnq_e - \frac{k_1 t}{2.303}$$

Pseudo- second-order kinetic: $$\frac{t}{q_t} = \frac{1}{k_2 q_e^2} + \frac{t}{q_e}$$

where q_e (mg/g) and q_t (mg/g) are the adsorption capacity at equilibrium and time t (min), respectively. k_1 (min^{-1}) and k_2 (min^{-1}) are the rate constant of pseudo-first-order and pseudo-second-order adsorption, respectively.

2. Theoretical Calculations

Quantum chemistry calculations are completed by the Gaussian 16 program[1]. The initial molecular structure is constructed in the GaussView program, and then directly imported into the Gauss 16 program. On the 6-31G* basis set, the B3LYP method based on density function theory is used to optimize its structure in the gas phase (using SDD pseudopotential and basis set for iodine), and all optimized structures have no virtual frequencies[2-4]. Then M062X/6-311+G** level was used to calculate the single point energy (using GD3 for dispersion correction, using SDD pseudopotential and basis set for iodine) [4,5], and the binding energy Eb is calculated as:

Eb=E(complex) -E(M)-E(I_2)

where E(complex) is the single-point energy of model molecules containing iodine, E(M) is the single-point energy of model molecules without iodine, and E(I_2) is the single point energy of iodine. Finally, the molecular electrostatic potential (ESP) analysis is completed by Multiwfn and VMD software packages [6-9].

3. Characterization

Fourier transform infrared spectroscopy (FT-IR, Bruker ALPHA II, Germany) characterization of the synthetic sample revealed the molecular structure and chemical bonds of the material in the 4000-450 cm^{-1} scanning range. The surface morphology of the samples was observed by scanning electron microscope (SEM, Hitachi SU8010, Japan) and transmission electron microscope (TEM, JEOL JEM-F200, Japan). The

crystalline structure of COFs was analyzed by X-ray diffractometer (XRD, Bruker D8 Advance, Germany). The chemical composition of the synthesized sample was analyzed by X-ray photoelectron spectroscopy (XPS, Thermo Scientific ESCALAB 250Xi, USA). Specific surface area and pore size analysis (BET, Micromeritics ASAP 2460, USA) were used to analyze the specific surface area and pore size distribution of the material. The structure information of COFs was investigated by ^{1}H-^{13}C Cross-polarized Magic Angle Rotation (CP-MAS) ^{13}C nuclear magnetic resonance spectroscopy (NMR, Bruker 400M, Germany). The absorbance of the solution was analyzed with an ultraviolet-visible spectrophotometer (Agilent UV-Vis Cary 60, USA).

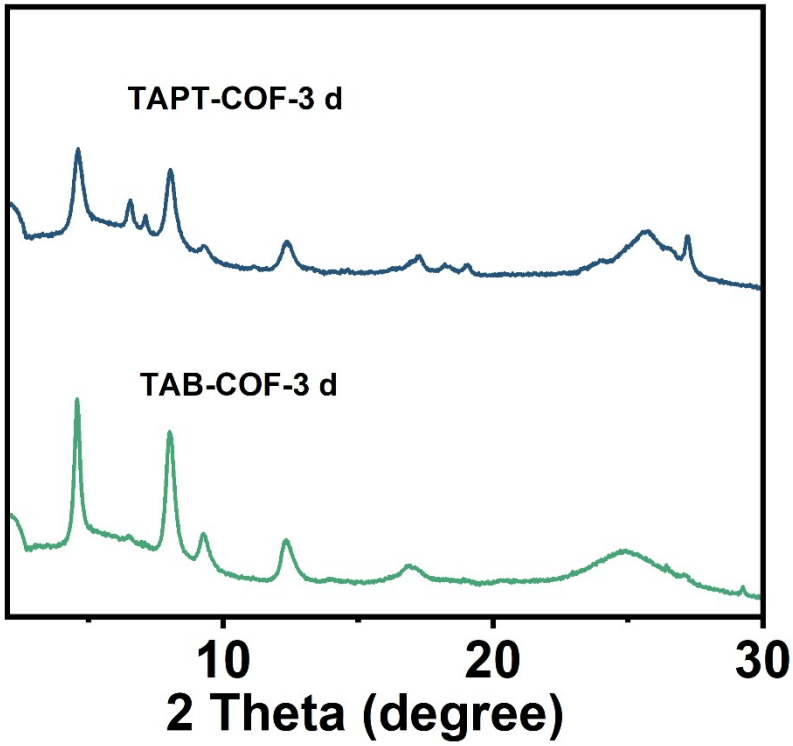

Fig S1. XRD pattern of TAPT-COF and TAB-COF synthesized for 3 days.

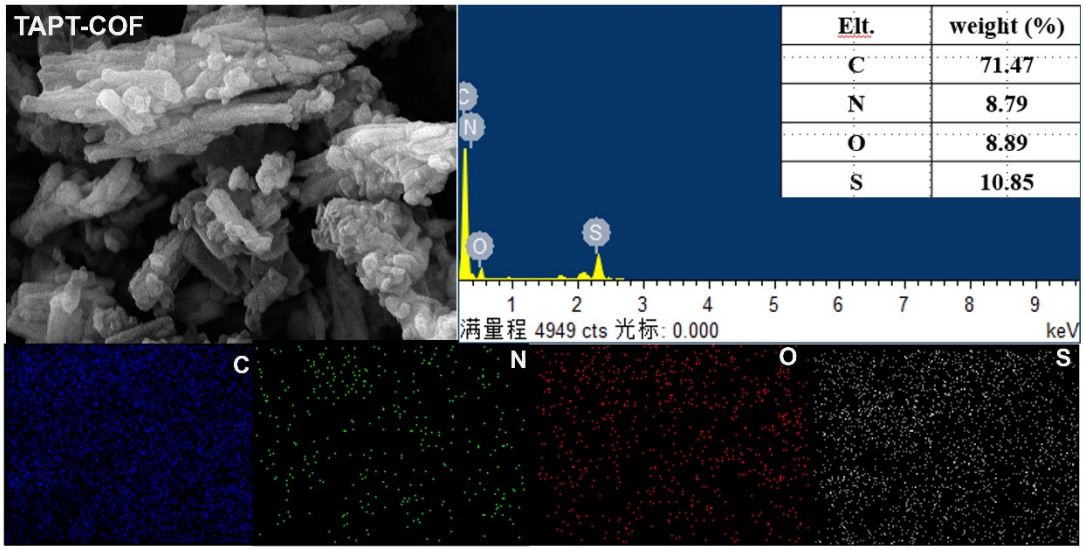

Elt.	weight (%)
C	71.47
N	8.79
O	8.89
S	10.85

Fig S2. Energy dispersive spectrometer images of TAPT-COF.

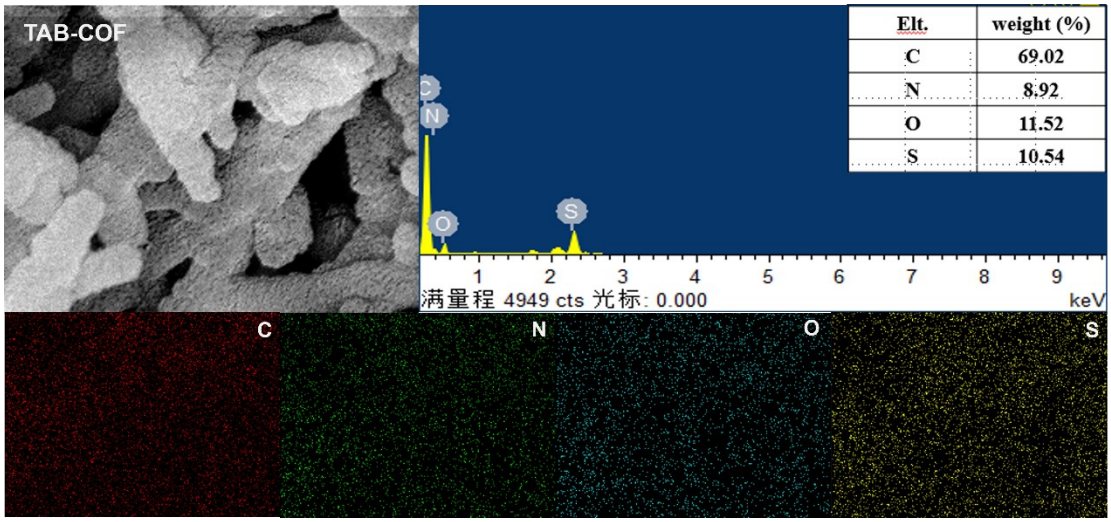

Elt.	weight (%)
C	69.02
N	8.92
O	11.52
S	10.54

Fig S3. Energy dispersive spectrometer images of TAB-COF.

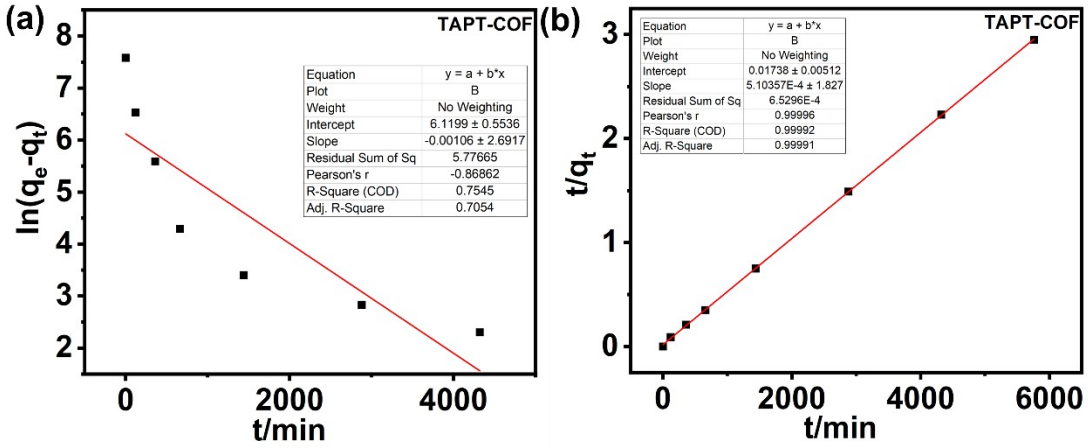

Fig S4. The fitting curves for (a) Pseudo-first-order and (b) pseudo-second-order kinetic model for the volatile iodine adsorption onto TAPT-COF.

Table S1. Kinetic parameters for the volatile iodine adsorption onto TAPT-COF.

q_e (exp)	Pseudo-first-order kinetic model			Pseudo-second-order kinetic model		
(mg^{-1})	k_1 (min^{-1})	q_e (mg/g)	R^2	k_2 (min^{-1})	q_e (mg/g)	R^2
1950	2.44×10^{-3}	454.82	0.7054	1.50×10^{-6}	1959.40	0.9999

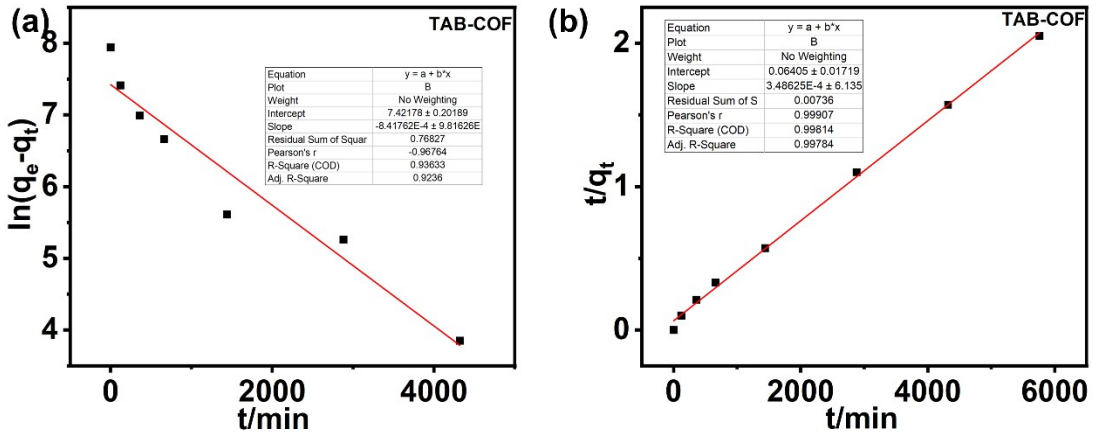

Fig S5. The fitting curves for (a) Pseudo-first-order and (b) pseudo-second-order kinetic model for the volatile iodine adsorption onto TAB-COF.

Table S2. Kinetic parameters for the volatile iodine adsorption onto TAB-COF.

q_e (exp)	Pseudo-first-order kinetic model			Pseudo-second-order kinetic model		
(mg^{-1})	k_1 (min^{-1})	q_e (mg/g)	R^2	k_2 (min^{-1})	q_e (mg/g)	R^2
2807	1.94×10^{-3}	1672	0.9236	1.90×10^{-6}	2868.41	0.9978

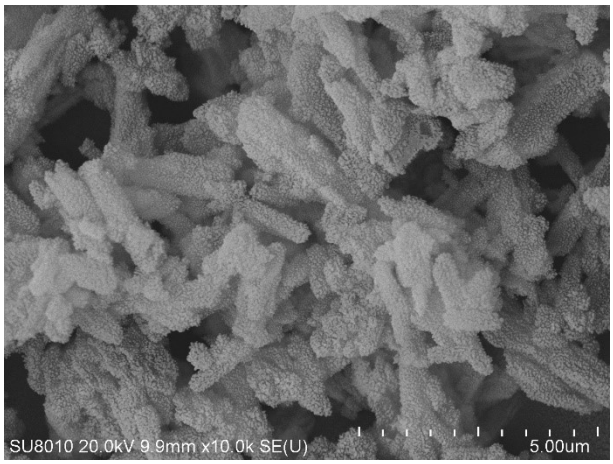

Fig S6. SEM images of I_2@ TAPT-COF.

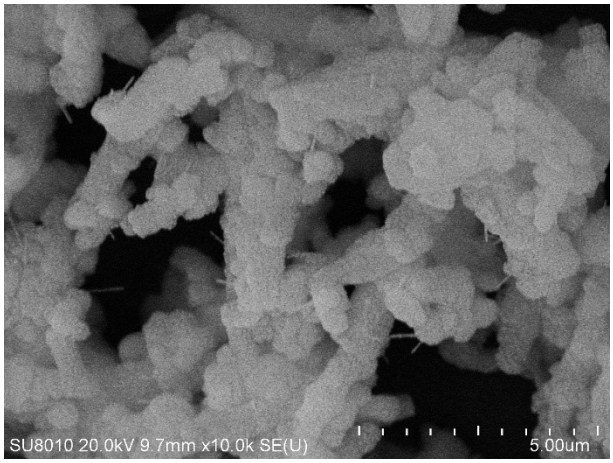

Fig S7. SEM images of I_2@TAB-COF.

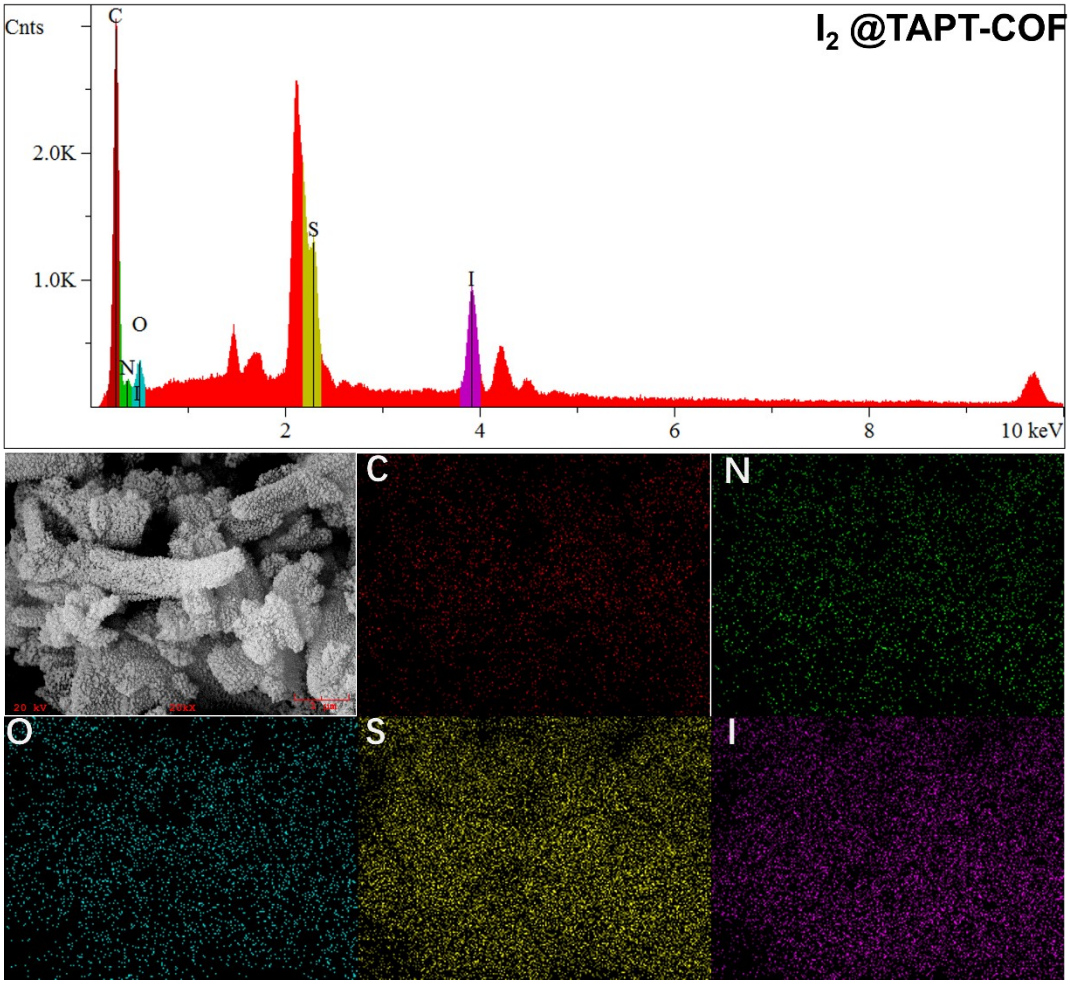

Fig S8. EDX analysis of I_2@TAPT-COF.

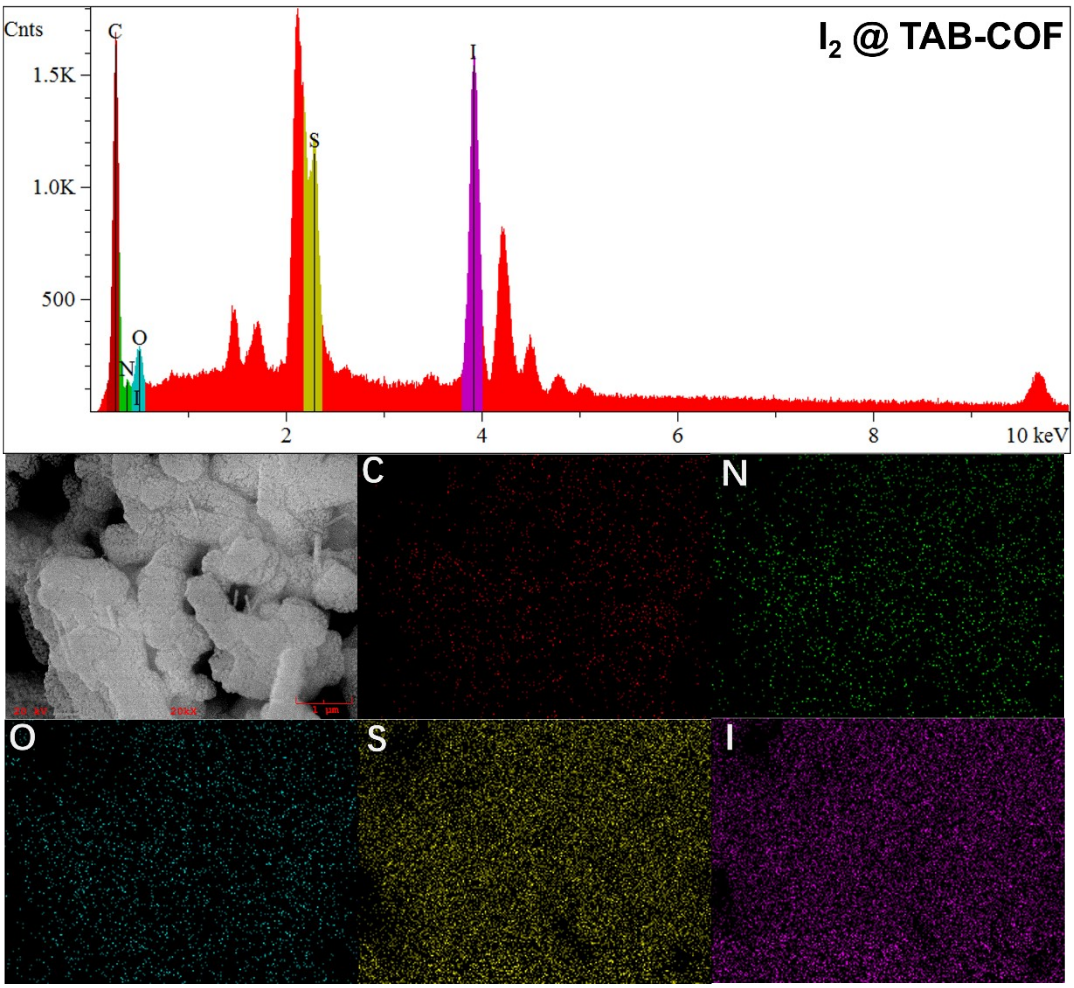

Fig S9. EDX analysis of I_2@TAB-COF.

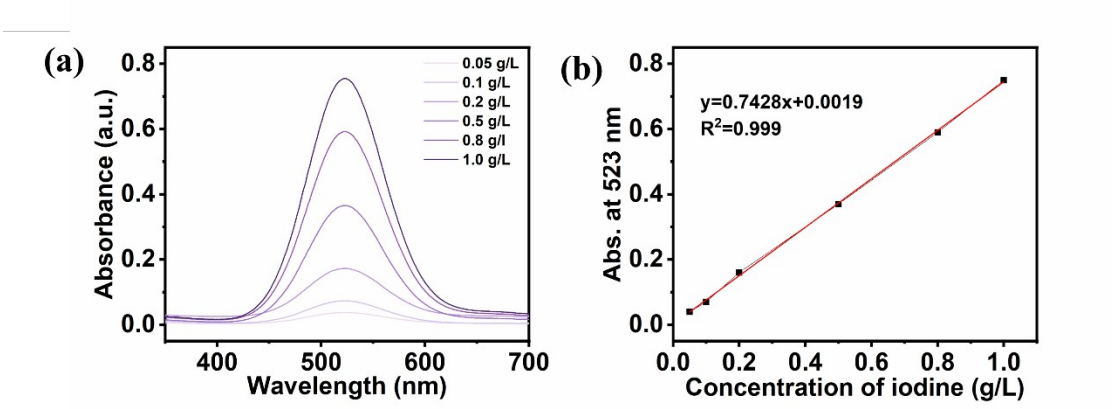

Fig S10. (a) Calibration plot of standard iodine by UV-visible spectra in cyclohexane solution. (b) The fitting of Abs value vs concentration of iodine in cyclohexane solution with the relatively good linearity satisfies Lambert-Beer Law.

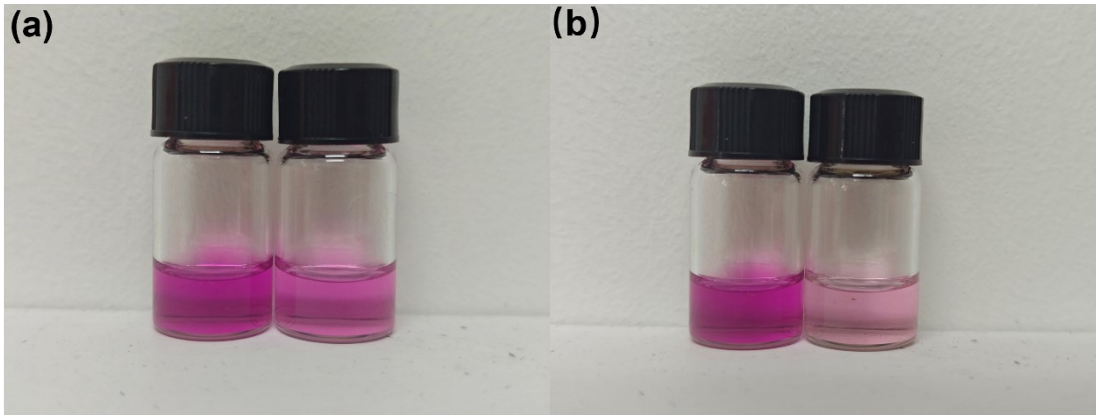

Fig S11. The photographs of a) TAPT-COF and b) TAB-COF pristine (left) and after (after) adsorption of iodine from cyclohexane solution.

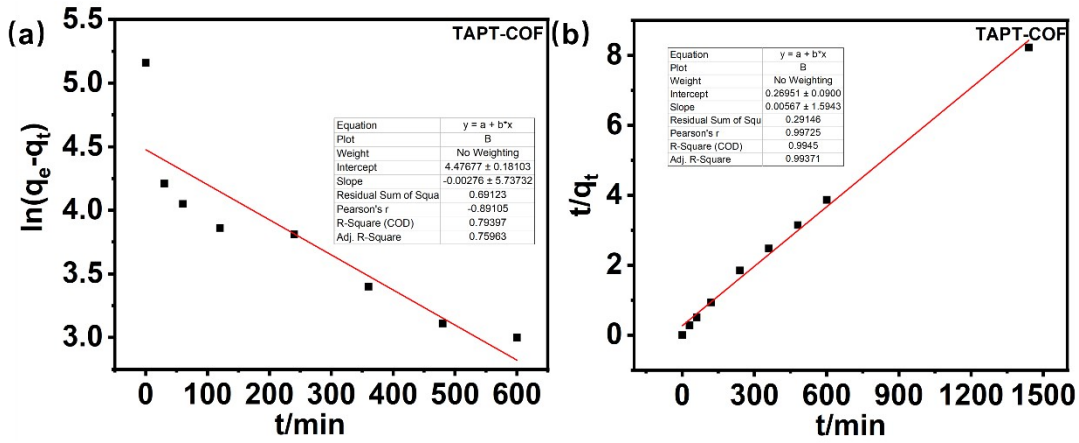

Fig S12. The fitting curves for (a) Pseudo-first-order and (b) pseudo-second-order kinetic model for the adsorption of iodine from cyclohexane solution onto TAPT-COF.

Table S3. Kinetic parameters for the adsorption of iodine from cyclohexane solution onto TAPT-COF.

q_e (exp)	Pseudo-first-order kinetic model			Pseudo-second-order kinetic model		
(mg^{-1})	k_1 (min^{-1})	q_e (mg/g)	R^2	k_2 (min^{-1})	q_e (mg/g)	R^2
175	6.36×10^{-3}	87.95	0.7596	1.19×10^{-4}	176.37	0.9937

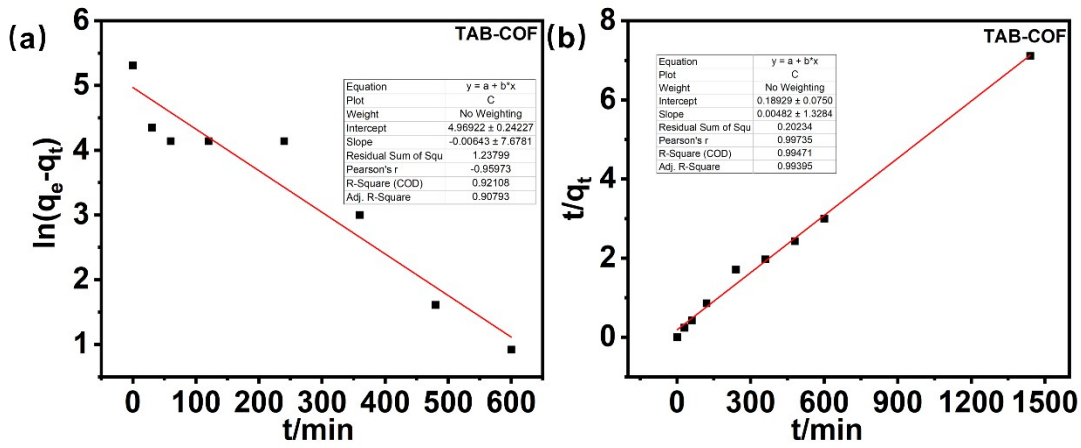

Fig S13. The fitting curves for (a) Pseudo-first-order and (b) pseudo-second-order kinetic model for the adsorption of iodine from cyclohexane solution onto TAB-COF.

Table S4. Kinetic parameters for the adsorption of iodine from cyclohexane solution onto TAB-COF.

q_e (exp)	Pseudo-first-order kinetic model			Pseudo-second-order kinetic model		
(mg^{-1})	k_1 (min^{-1})	q_e (mg/g)	R^2	k_2 (min^{-1})	q_e (mg/g)	R^2
200	1.48×10^{-2}	143.91	0.9210	5.18×10^{-3}	207.47	0.9947

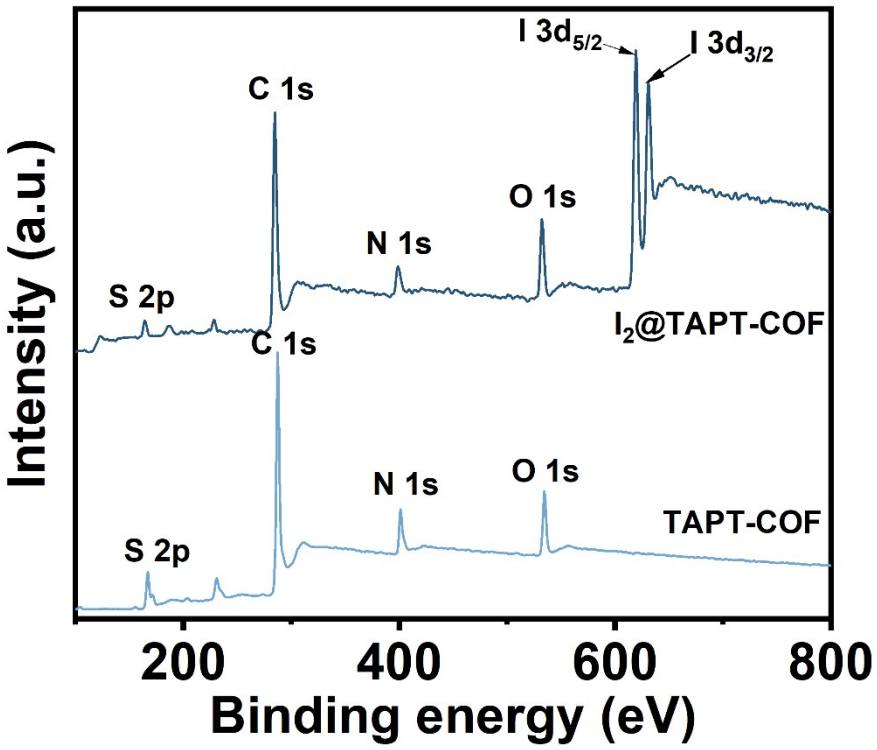

Fig S14. XPS spectra of TAPT-COF and I_2@ TAPT-COF.

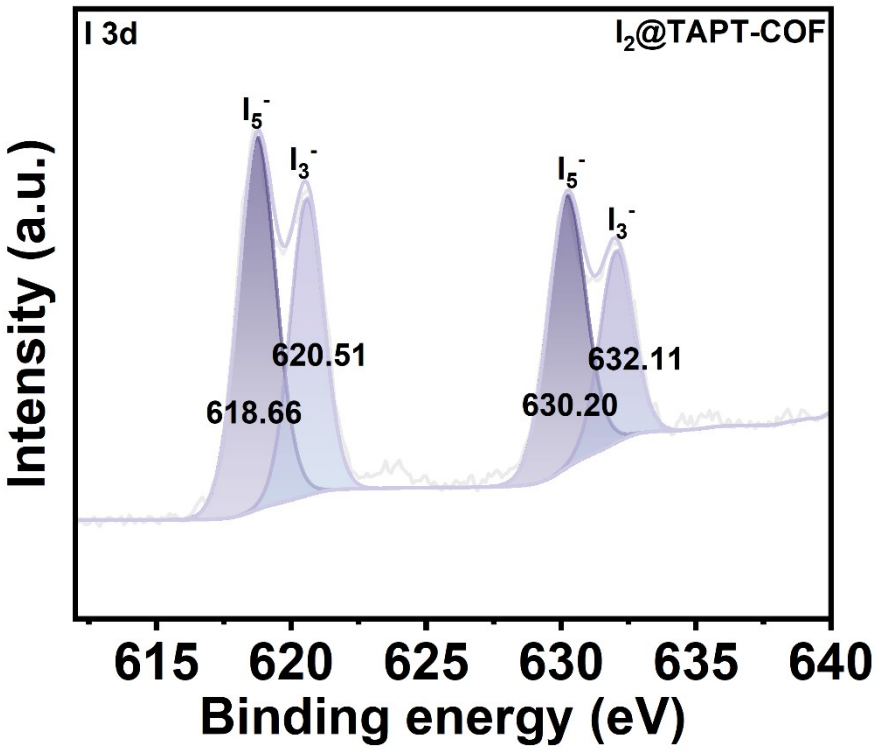

Fig S15. I 3d high-resolution XPS spectra of TAPT-COF and I_2@ TAPT-COF.

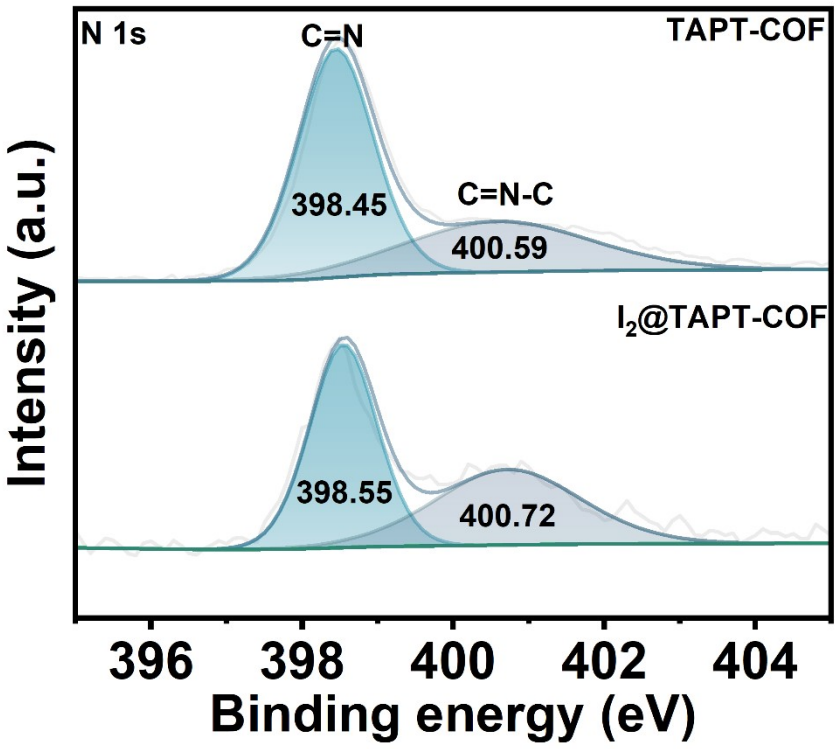

Fig S16. N 1s high-resolution XPS spectra of TAPT-COF and I_2@ TAPT-COF.

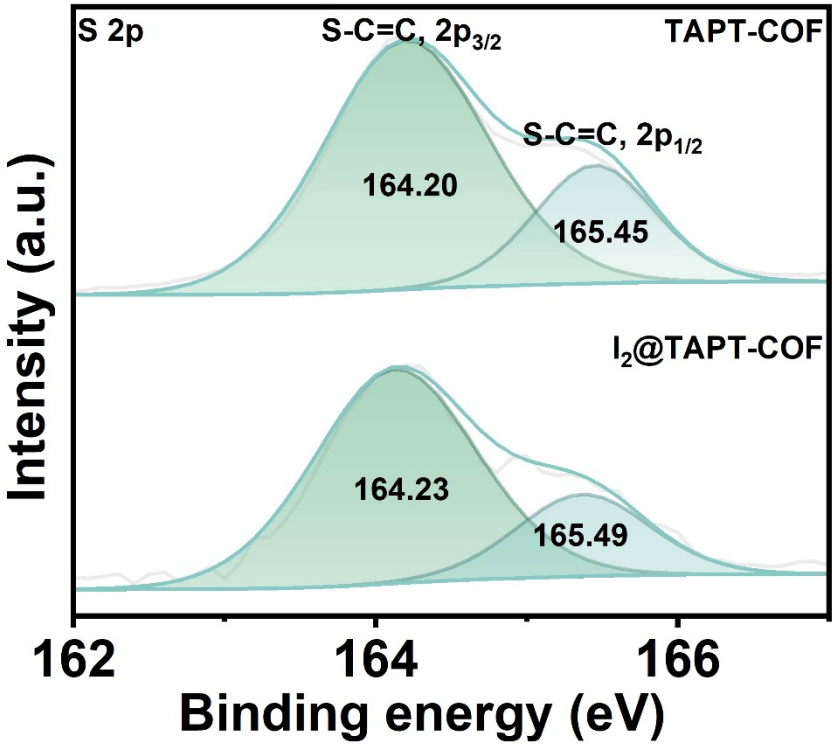

Fig S17. S 2p high-resolution XPS spectra of TAPT-COF and I_2@ TAPT-COF.

Table S5. Comparison of iodine adsorption capacities in different adsorbents.

Adsorbent	Temperature	I_2 uptake (g/g)	Ref.
MIL-53-TDC(In)	353 K	0.66	[10]
Th-UiO-66-$(NH_2)_2$	348 k	0.97	[11]
TAPT-COF	348 k	1.95	This work
SBA-15	333 K	2	[12]
3D-PPy	353 K	1.6	[13]
CuAceAd	353 K	0.61	[14]
TAB-COF	348 K	2.81	This work
BiZnAl-LDH	353 K	0.43	[15]
Cu-SBA-15	353 K	0.95	[16]
Th-UiO-66 MOF	353 K	0.97	[17]
TPP	353 K	2.47	[18]
POBI	348 K	2.29	[19]
Cu^0-MOF-303	353 K	0.84	[20]

[1]Frisch, M. J.,Trucks, G. W.,Schlegel, J.,Scuseria, G. E.,Robb, M. A.,Cheeseman, J. R.,Schlegel, H. B.,Scalmani, G.,Barone, V..Mennucci, B. Gaussian 09, Revision C.01.2010.
[2]Grimme, S.,Antony, J.,Ehrlich, S..Krieg, H. J. J. o. C. P. A consistent and accurate ab initio parametrization of density functional dispersion correction (DFT-D) for the 94 elements H-Pu.2010, 132 (15), 154104.
[3]Hehre.W., J. J. J. o. C. P. Self—Consistent Molecular Orbital Methods. XII. Further Extensions of Gaussian—Type Basis Sets for Use in Molecular Orbital Studies of Organic Molecules.1972, 56 (5), 2257.
[4]Lee, C.,Yang, W..Parr, R. G. Development of the Colle-Salvetti correlation-energy formula into a functional of the electron density.1988, 37 (2), 785.
[5]Lukehart, C. M. Computational Inorganic and Bioinorganic Chemistry.2007.
[6]Lu, T..Chen, F. J. J. o. C. C. O., Inorganic, Physical, Biological. Multiwfn: A multifunctional wavefunction analyzer.2012, (5), 33.
[7]Sdol, E. Journal of Molecular Graphics; Journal of Molecular Graphics, 2009.
[8]Zhang, J..Lu, T. J. P. C. C. P. Efficient evaluation of electrostatic potential with computerized optimized code.
[9]Lu, T..Manzetti, S. J. S. C. Wavefunction and reactivity study of benzo[a]pyrene diol epoxide and its enantiomeric forms.2014, 25 (5), 1521.
[10]Wang, L.,Li, T.,Dong, X.,Pang, M.,Xiao, S..Zhang, W. Thiophene-based MOFs for iodine capture: Effect of pore structures and interaction mechanism. Chemical Engineering Journal, 2021, 425, 130578.
[11]Fu, J.,Liu, J.-Y.,Zhou, Y.-R.,Zhang, L.,Wang, S.-L.,Qin, S.,Fan, M.,Tao, G.-H..He, L. A novel ionic-liquid-mediated covalent organic framework as a strong electrophile for high-performance iodine removal. Chemical Engineering Journal, 2024, 150913.
[12]Hijazi, A.,Azambre, B.,Finqueneisel, G.,Vibert, F.,Blin, J. L. High iodine adsorption by polyethyleneimine impregnated nanosilica sorbents. Microporous and Mesoprous Materials,2019, 288, 109586.
[13]A Sponge-Like 3D-PPy Monolithic Material for Reversible Adsorption of Radioactive Iodine.) Macromol. Mater. Eng. 2017, 302, 1700156.
[14] Flexible surface-supported MOF membrane via a convenient approach for efficient iodine adsorption. Journal of Radioanalytical and Nuclear Chenistry, 2020, 324 1167-1177.
[15]Dinh, T. D.,Zhang, D..Tuan, V. N. High iodine adsorption performances under off-gas conditions by bismuth-modified ZnAl-LDH layered double hydroxide. RSC Adv., 2020, 10, 14360-14367.
[16]He, X.,Chen, L.,Xiao, X.,Gan, Y.,Yu, J.,Luo, J.,Dan, H.,Wang, Y.,Ding, Y..Duan, T. Improved utilization of Cu0 for efficient adsorption of iodine in gas and solution by mesoporous Cu0-SBA-15 via solvothermal reduction method. Chemical Engineering Journal, 2023, 462, 142175.
[17]Li, Z. J.,Ju, Y.,Lu, H.,Wu, X.,Yu, X.,Li, Y.,Wu, X.,Zhang, Z. H.,Lin, J..Qian, Y. Cover Feature: Boosting the Iodine Adsorption and Radioresistance of Th-UiO-66 MOFs via Aromatic Substitution.Chem. Eur. J. 2021, 27, 1286-1291.

[18]Roja, A.,Srividhya, S..Arunachalam, M. Tripodal receptor cross-linked polymer as a promising adsorbent for iodine vapor capture and adsorption from water %J Polymer.2024, 294, 126688.
[19]Yang, M.,Shi, W.,Liu, S.,Xu, K. J. C.,Physicochemical, S. A..Aspects, E. Multifunctional diphenyl ether-based, cross-linked polyisocyanide for efficient iodine capture and NO2-/SO32-electrochemical probing.2022, 642, 128680.
[20]Li, M.,Wang, X.,Zhang, J.,Gao, Y..Zhang, W. J. A. S. S. Cu-loaded MOF-303 for iodine adsorption: The roles of Cu species and pyrazole ligands.2023, 619, 156819.